2019

Analysis of Gene Transcription Changes Following Chlamydia pneumoniae Infection of THP1 Monocytes May Have Relevance to Alzheimer's Disease

Desiré Guthier
Philadelphia College of Osteopathic Medicine

Philadelphia College of Osteopathic Medicine

Graduate Program in Biomedical Sciences

Department of Bio-Medical Sciences

Analysis of Gene Transcription Changes Following *Chlamydia pneumoniae* Infection of THP1 Monocytes may have relevance to Alzheimer's Disease

A Thesis in Biomedical Sciences by

Desiré Guthier

Submitted in Partial Fulfillment of the Requirements for the Degree of Master of Science in Biomedical Sciences 2019

We, the undersigned, duly appointed committee have read and examined this manuscript and certify it is adequate in scope and quality as a thesis for this master's degree. We approve the content of the thesis to be submitted for processing and acceptance.

Brian J. Balin, PhD.
Director of the Center for Chronic Disorders of Aging, Chair of the Department of Biomedical Sciences, Professor of Neuroscience and Neuropathology
Department of Bio-Medical Sciences
Thesis Advisor

Susan T. Hingley, PhD.
Professor of Microbiology
Department of Bio-Medical Sciences
Thesis Committee Member

Christopher Scott Little, PhD.
Associate Professor of Microbiology and Immunology
Department of Bio-Medical Sciences
Thesis Committee Member

Marcus G. Bell, PhD.
Director of the Graduate Program in Biomedical Sciences, Professor of Neuroscience, Physiology and Pharmacology
Department of Bio-Medical Sciences
Program Director, Master of Science in Biomedical Sciences, Research Concentration

ABSTRACT

Analysis of Gene Transcription Changes Following *Chlamydia pneumoniae* Infection of THP1 Monocytes may have relevance to Alzheimer's Disease

Desiré Guthier
M.S. in Biomedical Sciences, 2019
Dr. Brian J. Balin Ph.D., *Thesis Advisor*

There is increasing evidence that neuroinflammation caused by infectious agents is an important etiologic factor in neurodegenerative diseases including Alzheimer's disease (AD). One infectious agent that has been associated with AD is *Chlamydia pneumoniae* (*Cpn*). *Cpn* DNA can be detected within peripherally circulating mononuclear cells and there is evidence that infected mononuclear cells could be involved in chronic infection and contribute to inflammation at numerous anatomical sites, including the brain. Understanding *Cpn* genetic changes progressing from an acute to a chronic infection within monocytes may help to further elucidate the role of Cpn infected monocytes with regard to the neurodegeneration observed within AD. In this study, monocytes were infected in vitro with *Cpn* (either AR39 or CWL029) for 24, 48, 72, 96, or 120 hours. Subsequently, we investigated transcriptional gene changes of 7 *Cpn* genes using RT- PCR. We found a significant drop in gene expression at later time points in 3 of the genes. Our results demonstrate differences in gene expression from acute to chronic infection that perhaps indicate a trend towards persistence. However, our data does not unequivocally support that these gene changes are representative of the progression from acute to persistent infection. Future studies are required to resolve these differences and determine important gene changes that indicate persistent *Cpn* infection within monocytes.

TABLE OF CONTENTS

ABSTRACT.....iii

TABLE OF CONTENTS.....iv

LIST OF FIGURES AND TABLES vi

ACKNOWLEDGEMENTS.....vii

INTRODUCTION.....1

1.1 Hypothesis.....9

1.2 Specific Aims.....9

METHODS.....10

2.1 THP1 Human Monocytes.....10

2.2 Infection with *Cpn*.....10

2.3 RNA Isolation.....11

2.4 First Strand Synthesis.....12

2.5 Real Time- Polymerase Chain Reaction (RT-PCR).....12

2.6 Immunofluorescence.....13

RESULTS.....15

3.1 Qualitative evaluation of *Cpn* infection using immunofluorescent microscopy.....15

3.1.1 Determining percent infectivity using immunofluorescent labeling.....18

3.2 Cpn gene expression in human monocytes.....20

3.3 Normalization of Cpn gene transcription.....20

3.4 Cpn genes evaluated for transcriptional change.....20

DISCUSSION.....26

4.1 Conclusions.....31

REFERENCES.....33

APPENDIX.....38

5.1 Additional Material and Methods: DNA Isolation.....38

5.2 List of Appendix tables.....40

5.3 Additional Results.....41

5.3.1 *abcX* qRT-PCR raw data.....41

5.3.2 *euo* qRT-PCR raw data.....42

5.3.3 *l29* qRT-PCR raw data.....43

LIST OF FIGURES AND TABLES

Figure 1. Immunofluorescent labeling of AR39 Infected THP1 Monocytes..... 16

Figure 2. Immunofluorescent labeling of CWL029 Infected THP1 Monocytes. 17

Figure 3. Analysis of hctA gene expression of Cpn strain AR39 following infection of THP 1 Human Monocytes. 22

Figure 4. Comparative analysis of lcrH gene expression following infection of THP 1 Human Monocytes with two different Cpn strains AR39 and CWL029 23

Figure 5. Comparative analysis of tuf gene expression following infection of THP 1 Human Monocytes with two different Cpn strains AR39 and CWL029. 24

Figure 6. Comparative analysis of 16S gene expression following infection of THP 1 Human Monocytes with two different Cpn strains AR39 and CWL029 25

Table 1. Cpn genes examined and life cycle expression of those genes..... 8

Table 2. Percent infectivity using immunofluorescent labeling of AR39 infected THP1 monocytes..... 18

Table 3. Percent infectivity using immunofluorescent labeling of CWL029 infected THP1 monocytes..... 19

ACKNOWLEDGEMENTS

I would sincerely like to thank Brian J. Balin, PhD, my thesis advisor and mentor for his endless support, guidance, advice, expertise and patience throughout this project. I would also like to thank my committee members: Susan Hingley, PhD, and Christopher Little, PhD, for there continued guidance and providing me with important insight and feedback. Additional thanks to Susan Hingley, PhD who provided her unwavering support, expertise within the field, and technical skills in order to make this project possible. A special thanks to Chris Hammond, MS for her technical expertise for assistance in execution of all the experiments for this project. Without her guidance and advice this project would have not been possible. I would also like to acknowledge Marcus Bell, PhD, Director of the graduate program in Biomedical sciences for his encouragement and support. Finally, I would like to thank the Philadelphia College of Osteopathic Medicine (PCOM) community as a whole. PCOM has provided an academic environment in which I was able to thrive professionally and personally. PCOM has given me the opportunity to further pursue my professional goals as well as build lifelong relationships. The lessons I have learned at this institution I am truly grateful for and will bring forward with me throughout my personal and professional life.

INTRODUCTION

Alzheimer's Disease (AD) is a neurodegenerative disorder that currently affects an estimated 5.8 million Americans (1). As the population of the U.S., age 65 and older, continues to increase, this number is expected to escalate to 14 million by 2050 (1). In 2019, Americans will pay an estimated $290 billion on direct health care cost to care for those with AD and dementia (1). With statistics as stark as these, continued medical research into the etiology and pathogenesis of this disease is mandated.

Symptomatology of AD occurs on a progressive timeline; the beginning stage often presents as an insidious onset of short-term memory loss, altered mood, behavior, and impaired higher cognitive function, while later stages of the disease progress to incapacitating memory loss, disorientation, and eventually death (2). There are two known forms of Alzheimer disease: the early onset familial form (FAD) which accounts for ~5% of all AD cases and the late onset (LOAD) that accounts for the other ~95% of AD cases (3) . FAD is a genetic disease characterized by various mutations in one or more of the following genes, the amyloid precursor protein gene (APP), presenilin 1 gene, and the presenilin 2 gene (3). These mutations result in increased β- amyloid (Aβ) production and deposition extracellularly. A second defining neuropathological entity, the neurofibrillary tangles (NFTs), accumulate intracellularly within damaged neurons. Together, the two pathologies are the hallmark of AD. Unlike Familial AD, LOAD is not a result of genetic mutation. Environmental and genetic risk factors for LOAD have been identified (3), however, very little is known about the specific etiology and pathogenesis of this fatal disease.

There is controversy around the initiating factors of AD. One of the more widely accepted theories, coined the amyloid cascade hypothesis, involves the improper processing and cleavage of APP leading to Aβ production and deposition extracellularly (4). In both FAD and LOAD, Neurofibrillary tangles (NFTs) can accumulate intracellularly within damaged neurons (2). NFTs are made of the misfolded and hyperphosphorylated protein tau, a microtubule associated protein functioning normally as a structural and transport protein within the nerve cell. In the diseased state, the cell structure collapses and tau can no longer assist with the microtubule transportation of nutrients and neurotransmitters (2).

For the past two decades, Aβ plaques have been thought to initiate the pathological process of AD and be a significant contributor to neurotoxicity (5). However, this theory has been disputed for a number of reasons. For one, concentrations of plaques in the AD brain are in the picomolar range but given the amount of neurotoxicity displayed, the plaque concentrations would be expected to be a million times more concentrated in the micromolar range (6). Secondly, studies have shown through histochemical and immunocytochemical analyses, that numerous patients with Aβ amyloid deposition, examined postmortem, did not have symptoms of AD (7). This suggests that Aβ deposition may not necessarily be responsible for cognitive decline (7). Further, Aβ peptides may have neuroprotective effects by functioning as antimicrobial anionic defensive peptides (8). One more reason for disputing the amyloid hypothesis is clinical trial failures (9). Disease modifying drugs developed thus far have included drugs to reduce Aβ production, prevent Aβ aggregation, and drugs to promote Aβ clearance which have all demonstrated no efficacy and have failed phase III clinical trails (9).

Therefore, many questions remain unanswered about the true etiology and pathogenesis of LOAD, and as such, consideration of other evidence is warranted.

Inflammation in the brain in LOAD is a contributing factor to the neuropathology observed in AD. Activated microglia that respond to Aβ deposition and/or other insults may initiate and propagate an inflammatory response (6). Without complete clearance of the initiating stimuli, the cascade of neuroinflammation and neuropathology may be chronic (6). To date, clinical trials using NSAIDS as a method for treatment have proved ultimately unsuccessful (10). There has been some evidence to suggest that continued use of NSAIDs can delay onset of symptoms, but once cognitive dysfunction becomes apparent NSAIDs seem to have no effect (10-12).

Interestingly, another stimulus for neuroinflammation in AD may be infection (3, 13, 14). An infectious etiology for many chronic diseases, including AD, is not a foreign concept and has long been debated. Although infectious etiology of LOAD is not the standard dogma in the AD scientific community, there are many researchers around the world looking at infections as possible causative agents of LOAD. Prime examples of infectious agents being studied as potential pathologic causes of LOAD are Spirochetes (15), Herpes Simplex Virus 1(16, 17) and *Chlamydia pneumoniae (Cpn)* (3, 13, 14). *Cpn* is a very interesting potential etiologic agent of AD, and is the focus of this research study.

There is strong evidence to suggest a potential causal relationship between *Cpn* and LOAD. The first study correlating *Cpn* to AD was published in 1998 (18). The study looked at brain tissue samples from post- mortem LOAD patients as well as control brain tissue samples and used PCR with probes specific to *Cpn* DNA (18). Interestingly, 90%

of the postmortem brain tissues from AD patients were infected with *Cpn* in areas of the brain that usually exhibit AD pathology (18). This was compared to the control post-mortem brain tissue samples where only 5% of the brain tissue samples were determined to be infected with *Cpn* (18). The presence of *Cpn* in the AD brain the study used immunohistochemistry and electron microscopy techniques and results correlated with their initial PCR findings (18). The 1998 study also observed an interesting connection between ApoE e4 allele and *Cpn*, a noted risk factor for AD. Eleven out of the 19 cases that were infected with *Cpn* in the LOAD brain also had at least one ApoE ε4 allele (18). Additional evidence was obtained when non-transgenic BALB/c mice were intranasally infected with *Cpn*; Aβ deposits similar to plaques found in AD brains were found within the infected brains of the mice in areas typically affected in AD (19, 20).

Cpn is an obligate intracellular bacterium and is a pervasive respiratory pathogen (21). The acute infection with *Cpn* has a distinct developmental cycle that alternates between two morphological forms; the metabolically inactive and infectious form termed the elementary body (EB) and the metabolically active form responsible for repeated binary fission termed the reticulate body (RB) (21). After endocytic host cell entry, the EB converts to its metabolically active RB form and a specialized vacuole or inclusion body encapsulates the dividing bacteria (22). The RB are able to efficiently acquire nutrients from the host for fast replication and other metabolic activities within the host cell but are also not infectious and less stable than EBs at this point in their life cycle (23). The infection modifies host cell lysosomal pathways preventing lysosomal fusion with the vacuole, and the organism continues to multiply prior to conversion back to EBs for release from the cell and dissemination.

Cpn is airborne and is transmitted through respiratory droplets from person to person (24). *Cpn* is an etiologic agent for community acquired pneumonia and bronchitis (24) but has also been shown to disseminate throughout the body and may lead to exacerbation of atherosclerosis and possible involvement in AD etiology (18, 25). Furthermore, *Cpn* infection has also been associated with asthma (26), lung cancer (27), arthritis (28), chronic obstructive pulmonary disease (29), and diabetes (30). Potential modes of *Cpn* dissemination throughout the body have not been completely elucidated but there is strong evidence to suggest that the organism can move from the respiratory tract by a number of mechanisms. First *Cpn* can infect monocytes in the lung tissues and can travel systemically to many regions of the body (31). Of particular interest relating to AD, *Cpn* may enter the brain through the blood-brain barrier following infection of monocytes. Research has shown that *Cpn* infected monocytes can mitigate trans-endothelial entry through human brain microvascular endothelial cells (HBMECs) by up-regulation of VCAM-1 and ICAM-1 on HBMECs and increasing LFA-1, VLA-4, and MAC-1 on infected monocytes (31). This is an important discovery providing evidence on how *Cpn* could invade the brain to eventually promote inflammation characteristic of AD (31).

Another possible route for *Cpn* entry into the CNS is through the olfactory system. Since *Cpn* is a respiratory pathogen, it has ready access to olfactory neuroepithelium of the nasal olfactory system. Upon infection of these cells, the organisms could migrate to the olfactory bulbs and then to deeper areas of the brain such as the entorhinal cortex and hippocampus (32). Interestingly, an impaired sense of smell and olfactory dysfunction has been noted as an early dysfunction in AD (33).

Cpn has been reported to enter a chronic infectious state leading to persistence characterized by a long-term relationship between bacteria and infected host cells, including monocytes/macrophages (22). *Cpn* persistent infection is characterized by visualization through electron microscopy of enlarged, morphologically aberrant RBs that do not mature into infectious EBs (34, 35). Persistent infection may cause pathophysiology in chlamydial related diseases including AD (14, 36). For this reason, it is important to investigate causes of persistence and changes in *Cpn* gene expression during persistence to further understand host interaction. *Cpn* entering the persistent state as a response to stress is the current paradigm (36). Studies have been performed in which *Cpn* was driven into a persistent infection following exposure to antibiotics, interferon-ɣ (IFN- ɣ), and iron starvation(22, 37, 38) Intriguingly, current research suggests that *Cpn* persistence also may be a mechanism by which evasion of the host immune response through alternative metabolic pathways may occur (36).

As previously stated, although a specific etiology of LOAD pathogenesis has not been defined, evidence surrounding inflammation as a central contributing factor of LOAD pathology has been strongly suggested (39-42). In this regard, *Cpn*'s ability to maintain a chronic infection within monocytes has been shown to induce an inflammatory cascade (43). *Cpn* infection of monocytes in vitro has been shown to result in significant cytokine production including that of IL-1β, IL-6, and IL-8 (43). Thus if, *Cpn* infected monocytes cross the blood brain barrier, they have the potential to produce a significant inflammatory response that could lead to pathology seen in AD. How *Cpn* infection becomes chronic and/or persistent in monocytes to modulate the host immune response has not been fully elucidated. Genome wide *Cpn* analyses have been performed

within epithelial cells during an acute and induced persistent state to further understand *Cpn* and host interactions (22, 35, 44). Very few studies have looked at *Cpn* gene transcription within infected monocytes/ macrophages (34, 45).

Although *Cpn* Gene expression within monocytes is not well understood, it is crucial to the understanding of disease pathogenesis in which chronic or persistent infection is evident. Given the limited gene transcription analysis that has been performed within monocytes (22, 35, 44, 45), we examined the following *Cpn* genes; *euo*, *l29*, *abcX*, *tuf*, *hctA*, *lctH*, and *16S* (see table 1) within two different *Cpn* respiratory strains (AR39 and CWL029) to better understand *Cpn* gene expression following infection of human THP1 monocytes over a time course of 24-120 hours post infection (hpi).

Two common *Cpn* respiratory strains were chosen because it has been discovered that there are genetic differences between AR39 and CWL029, specifically 161/1165 proteins are not identical (46). Most importantly, there is a plasmid that is present in AR39 but not in CWL029 (46). For this reason, we wanted to determine if there is a difference in gene expression between AR39 and CWL029 following infection of monocytes. In addition, *Cpn* strains AR39 and CWL029 strains have been shown to be most closely related to the *Cpn* strains found in the AD brain and have also been shown to cause Aβ deposits similar to plaques in AD brains in mice (20).

hctA	Histone-like protein	Late cycle ~36 hpi (47)
lcrH	Chaperone protein within the T3SS	Late in cycle (47)
tuf	Elongation factor	Mid- late cycle (48)
16S	*Cpn* Ribosomal protein	Expressed throughout entire lifecycle
euo	Early upstream ORF	Early in cycle (49)
l29	50S ribosomal protein	Expressed throughout entire lifecycle (47)
abcX	ABC transporter ATPase	Expressed throughout entire lifecycle (47)

Table 1 Cpn genes examined and life cycle expression of those genes. In our study we examined the *Cpn* genes listed in the above table. These genes were chosen based on previous research showing evidence that these particular genes were expressed at variable time points in the *Cpn* life cycle (22). Gene expression profiles for *Cpn* have been previously defined in clusters. These clusters are defined by genes that are active at the same time in the life cycle: acute (24-48 hpi) and chronic (72-120 hpi) (22). We adopted this model in our study in order to further classify and choose genes of interest. In addition, each of these genes has shown to change its expression in a persistent state within an epithelial cell line (22).

1.1 Hypothesis

There will be gene transcriptional changes of *Cpn* following infection of human THP1 monocytes over a 120-hour time course that will reflect the evolution of an acute infection to that of a chronic infection independent of the *Cpn* strain (AR39 and CWL029) used for the infection.

1.2 Specific Aims

1. To analyze the percent of *Cpn* infected THP1 after 24, 48, 72, 96, and 120 hours post infection (hpi) with AR39 and CWL029 strains using immunofluorescent labeling techniques.
2. To evaluate changes of gene expression between acute (24-48 hpi) and chronic (72-120 hpi) stages of *Cpn* infection of THP1 monocytes in two strains of *Cpn* infection strain (AR39 and CWL029).
3. To determine if there is a difference in gene expression between AR39 and CWL029 infection strains over 24-120 hours post infection.

METHODS

2.1 THP1 Human Monocytes

THP1 monocytes were grown and maintained at $1x10^6$ cells/ml in RPMI growth media (GM) supplemented with heat activated 10% Fetal Bovine serum in an incubator at 37 °C and 5% CO_2.

2.2 Infection with *Cpn*

THP1 cells were centrifuged, washed with Hank's Balanced Salt Solution (HBSS), and then re-suspended at a concentration of $1x10^6$ cells/ mL in 1mL of GM. One of the two strains of human respiratory *Cpn,* AR39 or CWL029, were used to infect THP1 cells at Multiplicity of Infection (MOI) of 1. Cells were incubated at 37°C and 5% CO_2 for one hour in a T25 flask. GM was then added to the infected cells to bring the total volume of the flask up to 10mL. Cells were then incubated at 37°C and 5% CO_2 and infected THP 1 monocytes were extracted at 5 different time points: 24, 48, 72, 96 and 120 hours. Control experiments for all infected time points were performed with $1x10^6$ uninfected cells suspended in 10 mL of GM.

At the time of extraction for both infected samples and controls, T25 flasks were removed from the incubator and their contents were transferred into 25 mL tubes. The 25 mL tubes were centrifuged at 500 x g for 5 min. Supernatants were removed and pellets were washed with HBSS. Cell concentration was then determined using a hemocytometer and cell pellets consisting of $1x10^6$ cells were frozen at -60 °C until RNA extraction was performed for RT-PCR.

2.3 RNA Isolation

RNA was purified according to the manufacturer's instructions using a RNeasy isolation kit (Qiagen RNeasy). Frozen pellets were thawed and centrifuged for 5 min at 300 x g. Pellets contained $1x10^6$ cells for each sample. RLT (350 µl) was added to each sample to disrupt cells. This entire mixture was then pipetted into a QIAshredder placed in a 2ml collection tube. Sample was then centrifuged for 2 min at 20,000 x g to lyse cells. The QIAshredder was discarded and flow through in the collection tube was saved. 70% ethanol (350 µl) was added to the sample and mixed well. The entire volume was then transferred into a RNeasy spin column in 2 ml collection tube and centrifuged for 15s at 8000 x g. The flow through and collection tube were discarded and the RNeasy spin column was placed above a new collection tube. Buffer RW1 (350 µl) was added to the RNeasy spin column with collection tube and centrifuged for 15s at 8000 x g to wash the spin column membrane. Flow through was discarded and the RNeasy spin column was transferred into a new collection tube. DNase stock solution 1 (10 µl) was added to Buffer RDD (70 µl) and mixed thoroughly. DNase 1 incubation mix (80 µl) was added to RNeasy spin column membrane and the mixture was allowed to sit for 15 min to digest DNA. Buffer RW1 (350 µl) was added to the RNeasy spin column with collection tube and centrifuged for 15 sec at 8000 x g. Buffer RPE (500 µl) was added to the RNeasy spin column and centrifuged for 2 min at 8000 x g in order to wash the spin column membrane and dry any residual ethanol. The RNeasy spin column was then placed in a new collection tube and spun for 1 min at 20,000 x g to dispose of any carry over Buffer RPE. Flow through and collection tube were discarded. The RNeasy spin column was placed over a 1.5 ml collection tube. RNase free water (30 µl) was added to the RNeasy

spin column and centrifuged for 1 min at 8000 x g. This step was then repeated for a total of 60 µl of eluted RNA in RNase free water. Samples were frozen and stored at -60 °C until RNA was used for RT-PCR.

After RNA isolation was performed, overall RNA concentration was determined from its optical density at 260 nm by using UV Spectrophotometry. Other measurements recorded included purity values: A_{260}/A_{230} and A_{260}/A_{280}.

2.4 First Strand Synthesis

Reverse transcription reaction was performed using RETROscript Kit (Applied Biosystems) following manufacturer's protocol. RNA (500 ng) was mixed with 2 µl of Random Decamers; nuclease-free water was added to this mixture to total 12 µl. The mixture was then centrifuged briefly and heated for 3 min at 85 °C in order to denature RNA. Each sample was briefly centrifuged and placed on ice. Two µl of 10x RT buffer, 4 µl of dNTP mix, and 1 µl of RNase inhibitor was added to the denatured RNA sample. Samples were mixed thoroughly, centrifuged briefly, and incubated for 1 hour at 55 °C. Sample were then incubated for 10 min at 92 °C to inactivate the reverse transcriptase. Samples were then frozen and stored at -80 °C until cDNA was used for RT-PCR.

2.5 Quantitative Real-Time Polymerase Chain Reaction (qRT-PCR)

qRT- PCR was used to determine the relative level of gene transcription for the following genes: *euo*, *l29*, *abcX*, *tuf*, *hctA*, *lctH*, Human *18S* rRNA and chlamydial *16S*. qRT-PCR was run following manufacturer's protocol (Taqman Gene Expression Assay-Applied Biosystems) on *Cpn* infected THP1 monocytes and their uninfected controls for cDNA and DNA at 24, 48, 72, 96 and 120 hrs. For DNA samples, 10 µl of Master Mix, 1

µl of Primer, 250 ng of DNA, and DNase free water to equal 20 µl was added to each well of the 96- well plate. For cDNA samples 10 µl of Master Mix, 1 µl of Primer, 2 µl of cDNA, and DNase free water to equal 20 µl was added to each well of the 96- well plate. The qRT- PCR plate was run and analyzed using Applied Biosystems StepOne and StepOne plus Real-Time PCR systems. Expression of *Cpn* genes was normalized using human 18S rRNA as an endogenous control.

2.6 Immunofluorescence

Cpn labeling was visualized at 24, 48, 72, 96, and 120 hpi for both AR39 and CWL029 strains of *Cpn*. Cells at $1x10^5$ were suspended in 400µl of HBSS and pipetted into Shandon single Cytology Funnels (Fischer Scientific, Pittsburg, PA) with inserted Superfrost Slides (Fischer Scientific). Cytology Funnels containing slides and sample were centrifuged for 5 min at 500 rpm, medium acceleration, using a Shandon Cytospin III Cytocentrifuge. Cells were fixed onto slides with BD Cytofix/ Cytoperm for 30 mins, and washed with PBS at room temperature and immunolabeled with Cpn specific antibody (FITC directly tagged antibody 61C75, ThermoFischer) at 37°C for one hr. Slides were washed with filtered water and mounted with Flouro-gel II Mounting medium with DAPI and coverslips. Slides were stored at 4°C without light until visualization.

Samples were viewed using a Nikon Eclipse 80i microscope 40x Nikon Plan Flour 40x/0.75 OFN25 DIC M/N2 objective. For each slide, 10 fields were captured using Nikon DS- Ri1 Camera and NIS- Elements Advanced Research Software version 3.0 (Nikon). For each field captured, total cell counts and *Cpn*-infected cell counts were

documented. Criteria for positive cell count required visualization of three or more punctate bodies or 1 large inclusion. Percentage of infected cells were determined from these counts at each time point. Experiments were performed in triplicate and counts were averaged for statistical significance.

RESULTS

3.1 Qualitative evaluation of Cpn infection using immunofluorescent microscopy

Cultures of THP1 monocytes infected with *Cpn* strains CWL029 and AR39 for 24, 48, 72, 96, or 120 hrs were evaluated for percent infectivity using immunofluorescent microscopy analysis. Figure 1 shows representative micrographs of AR39 infected THP1 monocytes at 24, 48, 72, 96, and 120 hours post-infection (hpi) and uninfected control cells. The percent infected at 24, 48, 72, 96, and 120 hpi were 52.4 ± 1.0%, 47.0 ± 1.8%, 53.9 ± 4.0%, 46.6 ± 2.8, and 48.3 ± 4.1%, respectively (see table 2). The uninfected THP1 monocytes showed 0% infectivity for all time points. Figure 2 shows representative micrographs of CWL029 infected THP1 monocytes at 24, 48, 72, 96, and 120 hpi and uninfected control groups. The percentage of cells infected at 24, 48, 72, 96 and 120 hpi were 41.3% ± 1.7, 45.0% ± 4.5, 55.6% ± 4.7, 61.8% ± 4.7, and 62.7 ± 2.6%, respectively (see table 3). The uninfected THP1 monocytes showed 0% infectivity for all time points.

Figure 1. Immunofluorescent labeling of AR39 Infected THP1 Monocytes.

At all-time points, 24-120 hours uninfected cells were immunolabeled for *Cpn* and shown to be negative for infection (representative micrograph, A). THP1 Monocytes infected for 24, 48, 72, 96, and 120 hpi demonstrated Cpn (green) respectively (B-F). Cell nuclei in all micrographs were labeled with DAPI (blue). Original magnification (400x).

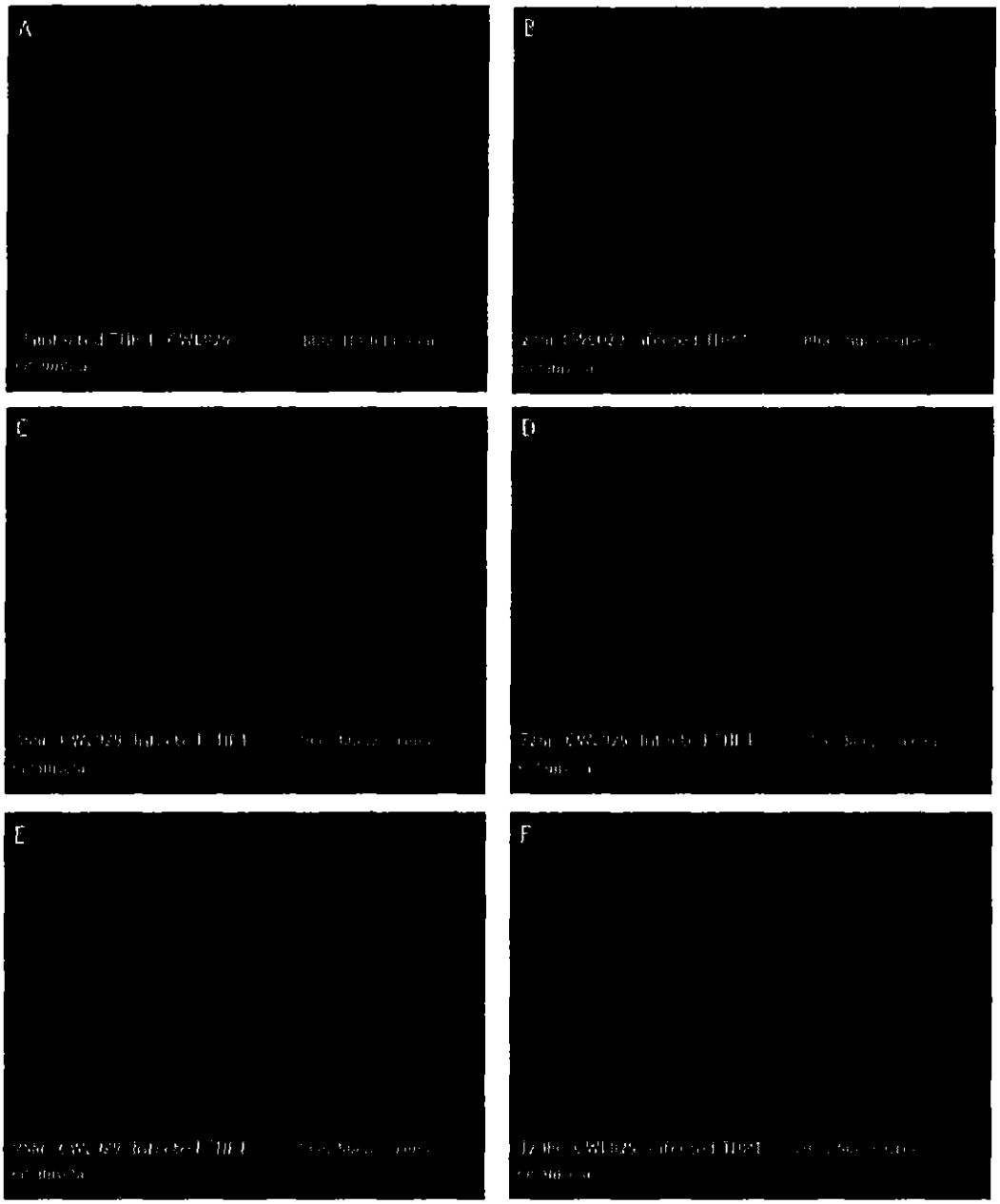

Figure 2. Immunofluorescent labeling of CWL029 Infected THP1 Monocytes. At all time points, 24-120 hours uninfected cells were immunolabeled for *Cpn* and shown to be negative for infection (representative micrograph, A). THP1 Monocytes infected for 24, 48, 72, 96, and 120 hpi demonstrated Cpn (green) respectively (B-F). Cell nuclei in all micrographs were labeled with DAPI (blue). Original magnification (400x).

3.1.1 Determining percent infectivity using immunofluorescent labeling

AR39	Biological Replicates	Total # of Cells Positive	Total # of Cells Counted	Percent Infected	Percent Totals
24 hpi	Experiment 1	60	113	53.1	52.4 ± 1.0
	Experiment 2	60	125	51.2	
	Experiment 3	54	102	52.9	
48 hpi	Experiment 1	56	124	45.2	47.0 ± 1.8
	Experiment 2	62	127	48.8	
	Experiment 3	56	119	47.1	
72 hpi	Experiment 1	55	105	52.4	53.9 ± 4.0
	Experiment 2	95	187	50.8	
	Experiment 3	122	209	58.4	
96 hpi	Experiment 1	56	129	43.3	46.6 ± 2.8
	Experiment 2	84	174	48.3	
	Experiment 3	102	212	48.1	
120 hpi	Experiment 1	49	96	51.0	48.3 ± 4.1
	Experiment 2	89	177	50.3	
	Experiment 3	80	184	43.5	

Table 2. Percent infectivity using immunofluorescent labeling of AR39 infected THP1 monocytes.

At all-time points, 24-120 hours uninfected cells were immunolabeled for *Cpn* and shown to be negative for infection (cell counts not shown). THP1 monocytes infected for 24-120 hpi were immunolabeled for *Cpn*. For each experiment, 10 fields were captured using Nikon DS- Ri1 Camera and NIS- Elements Advanced Research Software version 3.0 (Nikon). Criteria for positive cell count required visualization of three or more punctate bodies or 1 large inclusion.

CWL029	Biological Replicates	Number of Cells Positive	Total cells Counted	Percent Infected	Percent Totals
24 hpi	Experiment 1	50	124	40.3	41.3 ± 1.7
	Experiment 2	56	139	40.3	
	Experiment 3	77	178	43.3	
48 hpi	Experiment 1	59	121	48.8	45.0 ± 4.5
	Experiment 2	97	210	46.2	
	Experiment 3	69	172	40.1	
72 hpi	Experiment 1	83	160	51.9	55.6 ± 4.7
	Experiment 2	72	133	54.1	
	Experiment 3	98	161	60.9	
96 hpi	Experiment 1	81	121	66.9	61.8 ± 4.7
	Experiment 2	99	172	57.6	
	Experiment 3	178	292	61	
120 hpi	Experiment 1	125	198	63.1	62.7 ± 2.6
	Experiment 2	102	157	65	
	Experiment 3	91	152	59.9	

Table 3. Percent infectivity using immunofluorescent labeling of CWL029 infected THP1 monocytes.

At all-time points, 24-120 hours uninfected cells were immunolabeled for *Cpn* and shown to be negative for infection (cell counts not shown). THP1 monocytes infected for 24-120 hpi were immunolabeled for *Cpn*. For each experiment, 10 fields were captured using Nikon DS- Ri1 Camera and NIS- Elements Advanced Research Software version 3.0 (Nikon). Criteria for positive cell count required visualization of three or more punctate bodies or 1 large inclusion.

3.2 Cpn gene expression in human monocytes

We analyzed the transcription of 7 *Cpn* genes expressed by two different strains (AR39 and CWL029) of *Cpn* in THP 1 monocytes. Cells were lysed and RNA was extracted at 24, 48, 72, 96, and 120 hpi. Amplification of RNA from uninfected monocytes was included as negative control. Forty-eight hpi was used as a reference time point and *18S* rRNA was used as a human housekeeping gene to normalize transcription levels. RT reaction used cDNA, which was then used in RT-PCR. Relative quantities of transcribed genes were obtained using qRT-PCR. All genes were evaluated in triplicate per PCR plate and each gene was amplified on multiple PCR plates.

3.3 Normalization of Cpn gene transcription

Human *18S* rRNA was used to normalize the *Cpn* transcription data. We initially used chlamydial *16S* rRNA to normalize chlamydial expression as numerous published articles have used this gene as a housekeeper gene (22, 44, 50). However, during our study we found that although *16S* was stably expressed at each time point, there was variability between the time points. Human *18S* rRNA was the most stably expressed gene we analyzed as the CT value for the expression was consistent regardless of time point. This allowed us to compare Cpn expression levels to total gene expression in the cell making it the best candidate for a control in our experiments.

3.4 Cpn genes evaluated for transcriptional change

Expression of *hctA* of *Cpn* for strain *AR39* had a 2.6 fold increase from 24 to 48 hpi. Gene expression continued to increase and peaked at 72 hours. A 3.5 fold decrease

gene expression was observed from 72 to 96 hpi and remained low at 120 hpi. The same gene in the CWL029 strain showed no difference (Figure 3).

Cpn lcrH transcription levels for strain AR39 were elevated at 72 hpi in comparison to the other time points. A 2.4 fold increase from 48 hpi to 72 hpi is seen in the AR39 *Cpn* strain. In contrast, CWL029 *lcrH* transcription levels decreased by 2.3 fold from 48 hpi to 72 hpi. Both strains showed transcription levels decreasing at 96 hpi and 120 hpi. AR39 *lcrH* transcription levels decreased 6.5 fold from 48 hpi to 72 hpi. CWL029 *lcrH* transcription levels decreased 1.8 fold from 48 hpi to 72 hpi (Figure 4).

Our data for *Cpn* AR39 *tuf* gene expression showed highest transcriptional levels at 24 hpi by 3.24 fold when compared to 48 hpi. Decreased levels of transcription by 3.9 fold were observed at both 96 hpi and 120 hpi when compared to 48 hpi. *Cpn* CWL029 had much lower transcriptional levels at almost every time point, although, a similar pattern to the AR39 strain was observed for 48-120 hpi (Figure 5).

Cpn AR39 *16S* rRNA expression interestingly shows transcription levels are 2.4 fold higher at 24 hpi and 1.7 fold higher at 72 hpi when compared to 48 hpi. Transcription levels then decrease by 1.16 fold at 96 hpi when compared to 48 hpi. Transcription levels of *16S* rRNA for *Cpn* CWL029 were lower at 24, 72, 96 and 120 hpi when compared to 48 hpi. Transcription levels were decreased by 3.2 fold and 5.4 fold at 96 hpi and 120 hpi, respectively when compared to 48 hpi (Figure 6).

Data for *euo, l29* and *abcX* gene expression also was collected for both strains, however standard deviations were too high to make any conclusions (raw data in appendix).

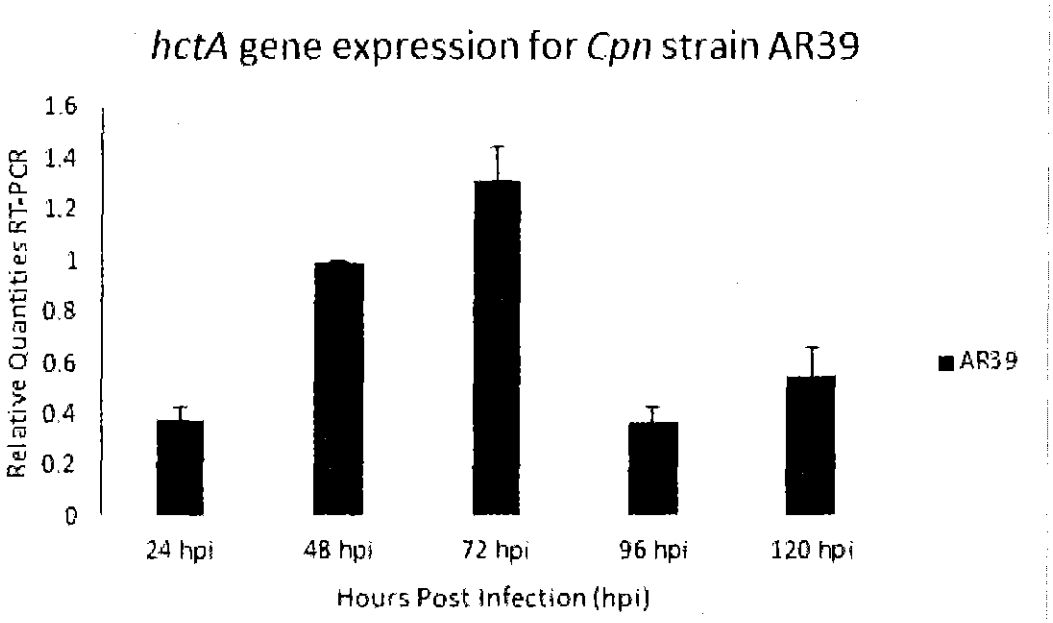

Figure 3. Analysis of *hctA* gene expression of *Cpn* strain AR39 following infection of THP 1 Human Monocytes. Cells were infected (MOI 1, n=12) with *Cpn* and relative expression of *hctA* was quantified at 24, 48, 72, 96, and 120 hpi. 48 hpi was used as a reference time point and *18S* was used as an endogenous control. Data for the CWL029 strain was collected but not shown as there was not a change at any time point. n=number of technical replicates from same sample. Error bars represent standard deviations.

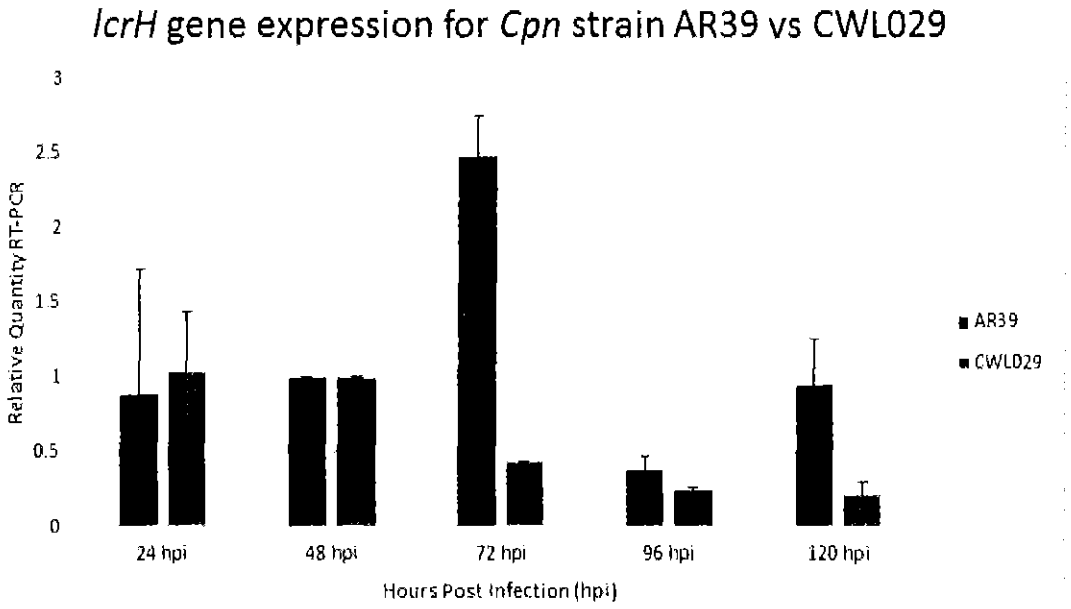

Figure 4. Comparative analysis of *lcrH* gene expression following infection of THP 1 Human Monocytes with two different *Cpn* strains AR39 and CWL029. Cells were infected separately (MOI 1) with *Cpn* (AR39, n=9 and CWL029, n=6) with *Cpn* and relative expression of *lcrH* was quantified at 24, 48, 72, 96, and 120 hpi. 48 hpi was used as a reference time point and *18S* was used as an endogenous control. n= number of technical replicates from same sample. Error bars represent standard deviations.

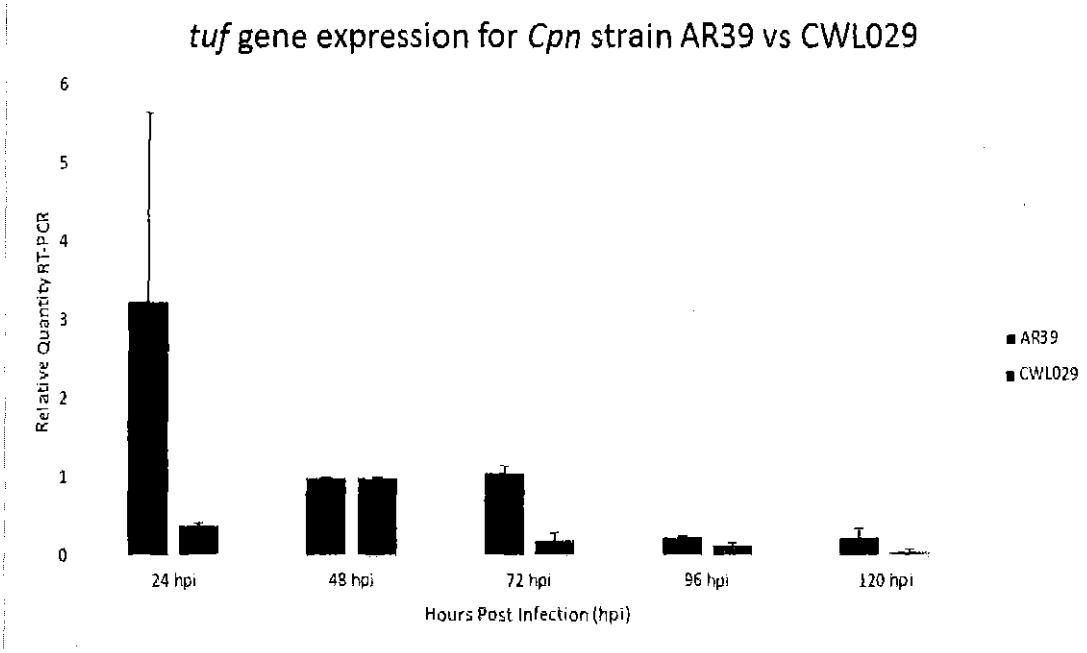

Figure 5. Comparative analysis of *tuf* gene expression following infection of THP 1 Human Monocytes with two different *Cpn* strains AR39 and CWL029. Cells were infected separately (MOI 1) with *Cpn* (AR39, n= 6 and CWL029, n=6) with *Cpn* and relative expression of *tuf* was quantified at 24, 48, 72, 96, and 120 hpi. 48 hpi was used as a reference time point and *18S* was used as an endogenous control. n= number of technical replicates from same sample. Error bars represent standard deviations.

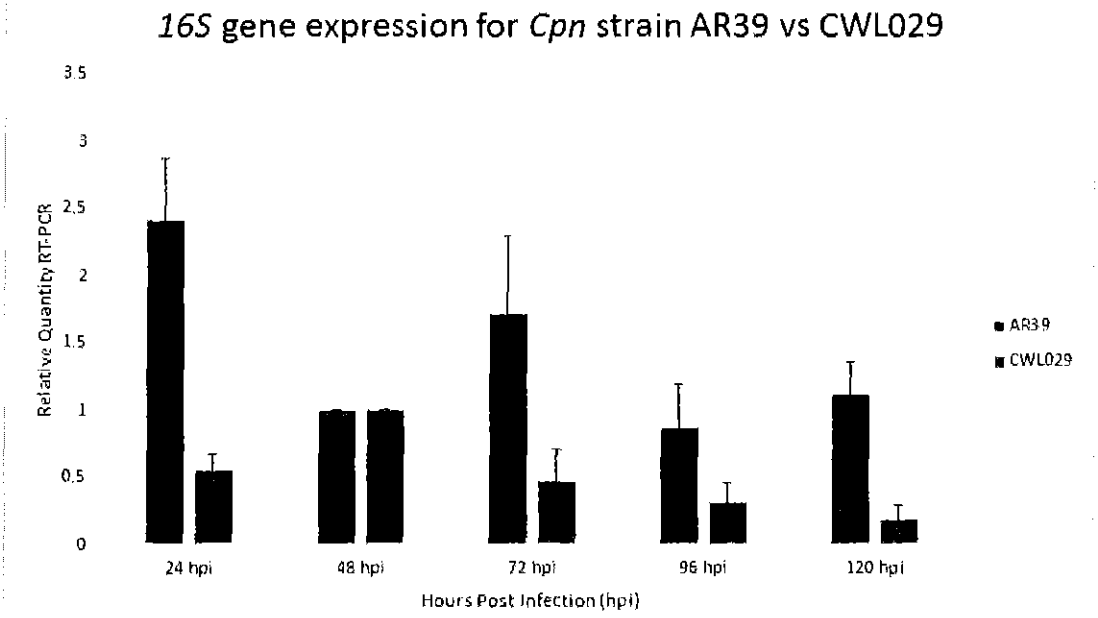

Figure 6. Comparative analysis of *16S* gene expression following infection of THP 1 Human Monocytes with two different *Cpn* strains AR39 and CWL029. Cells were infected separately (MOI 1) with *Cpn* (AR39, n=15 and CWL029, n=12) with *Cpn* and relative expression of *lcrH* was quantified at 24, 48, 72, 96, and 120 hpi. 48 hpi was used as a reference time point and *18S* was used as an endogenous control. n= number of technical replicates from same sample. Error bars represent standard deviations.

DISCUSSION

Previous studies have identified and analyzed transcriptional changes during the developmental life cycle of *Cpn* during acute infection (22, 51, 52). Genome wide transcriptional analyses have mostly been reported within epithelial cell lines (22, 35, 44), and while these studies have been monumentally important in understanding the life cycle of *Cpn,* changes in gene expression within white blood cells is essential for a more complete understanding of disease pathogenesis of AD. The monocyte is an important link between acute and chronic infection with *Cpn* because of Cpns ability to maintain a persistent state within the cell and cause the host cell to elicit a chronic inflammatory response (43). In this regard, only a few studies have explored transcriptional gene changes within monocytes (34, 45). In the current study, we have explored transcriptional changes of *Cpn* within THP1 monocytes in vitro to determine how gene changes are regulated in a temporal pattern as the infection progresses.

Cpn replicates within a eukaryotic host cell in a unique developmental cycle marked by EB and RB. The lifecycle of Cpn is marked by temporal genes that are expressed during early, mid and late stages of the life cycle and in times of stress enter into a persistent state (22). In the current study, we have evaluated the transcriptional levels of Cpn genes at different time points of the Cpn lifecycle. For example, *hctA* is a gene for Histone H1 like protein with homology to eukaryotic histone protein (54). *HctA* has been proposed to be essential for differentiation from RB back to EB (55). During acute infection, the gene is expressed in the late phase of the acute life cycle; previous studies have shown increased transcriptional activity at 36 hpi during a 48 hour *Cpn*

lifecycle (22). Expression of this histone like protein represses further transcription and translation of the chlamydial genome (54, 56). In our study, following infection with the AR39 strain of *Cpn,* the relative quantity of *hctA* more than doubled from 24 to 48 hours and gene expression peaked at 72 hpi. These results are consistent with previous studies showing increased expression in late phase of the life cycle. Unexpectedly, we found that at 96 hpi and 120 hpi there was a significant drop in gene expression of *hctA*. Decreased expression of *hctA* could possibly represent a trend towards persistence in monocytes. However, previous studies have demonstrated conflicting data for expression of *hctA* during persistence. One study demonstrated that depletion of iron lead to persistence and *hctA* gene expression was unaltered during this state (22). In contrast, two studies demonstrated that during penicillin induced persistence, down regulation of *hctA* expression occurred (44, 57). Further, IFN-γ models of persistence have shown both up regulation of *hctA* (44) as well as down regulation of *hctA* (36). Variations in expression of this gene could possibly be explained by the different conditions promoting persistence in these models, however this correlation remains to be clarified.

Cpn gene analysis demonstrated that at 96 hpi and 120 hpi, the *tuf* gene was downregulated significantly when compared to earlier time points. *Tuf* is a gene that transcribes for an elongation factor that is highly conserved among eubacteria (58). *Tuf* has been shown to be expressed during mid and late cycle with complex regulation (48). Interestingly, this gene has also been used in previous studies as a housekeeping gene following infection of epithelial cells (22). In our study we saw a drop-in gene expression over time. Down regulation of *tuf* at later time points could indicate a decrease in translational activity and potentially indicate a trend toward *Cpn* persistence within

monocytes. Confirmation of this persistence could be obtained upon visualizing persistent aberrant bodies with ultrastructural analysis, which unfortunately was outside the scope of the current study. Also, it would be interesting to see if similar results would be obtained upon inducing persistence with methods such as exposure to IFN-γ or iron depletion.

Surprisingly, we found differences in gene expression between *Cpn* strains AR39 and CWL029. When evaluating AR39 at 72 hpi, *lcrH* had increased expression from 48 hpi. When evaluating CWL029 there was a decrease in gene expression from 48 hpi. *LcrH* is a gene that expresses a chaperone protein within the *Cpn* Type III secretion system (T3SS), an important virulence factor that allows interaction between bacterium and host. Bacteria use T3SS to inject proteins into the host cell cytosol changing the environment in favor of bacterial survival (59). This could suggest that there may be strain differences in expression of the T3SS. Since the T3SS changes the environment of the host cytosol, differences in gene expression could potentially alter the expression of multiple proteins.

Interestingly, with both the CWL029 and AR39 *Cpn* strains there was down regulation in the *lcrH* gene expression at 96, and 120 hpi. These findings are consistent with previous studies, which have shown decrease in *lcrH* gene expression during persistent infections. IFN-γ mediated persistence as well as iron depletion mediated persistence has demonstrated down regulation of gene expression (22, 44, 60). Although we are not able to specifically determine persistence in our study, decreased transcription

of *lcrH* during later timer points is interesting as it is consistent with downregulation of gene transcription in iron depletion of *Cpn* which leads to persistence (22).

One interesting finding that we discovered is that *Cpn 16S* was not the best housekeeping gene for normalization, although, several previous studies normalized *Cpn* gene expression to *Cpn 16S* (22, 44, 50). However, another study found similar results to ours in that *16S* rRNA produced higher standard deviations compared to other housekeeping genes (22). Subsequently, we found that THP1 eukaryotic *18S* was the most stably expressed housekeeping gene in our study. This raises an important question on choosing the best gene candidates for PCR normalization in any given experimental design, and whether or not *16S* should be used routinely as a housekeeping gene.

Cpn immunofluorescent data for the AR39 strain showed approximately 46-53% percent infectivity at 24-120 hpi. *Cpn* immunofluorescent data for the CWL029 strain showed approximately 41-62% percent infectivity at 24-120 hpi. We infected THP1 monocytes at an MOI= 1. However, multiple infectious units were present within THP1 monocytes and no infectious units were present in other cells. We believe that the same number of infectious units were present in our experiment but did not infect the cells in a 1:1 ratio. Overall the infectivity of the THP1 monocytes stayed relatively uniform from 24-120 hpi for both *Cpn* strain AR39 and CWL029. Our infection was maintained at the same percent infectivity throughout 24 hpi-120 hpi and there was overall decrease in gene transcription of the Cpn genes evalutated. This could potentially indicate a trend toward a persistent infection since the infection is being maintained through 120 hpi at around the same percent infectivity as the early time points and transcriptional levels are

decreasing. However, it is unclear weather or not the infection we are visualizing at the chronic time points (after 48 hpi) could also represent a recycling of an acute infection. These results would need to be confirmed with visualization on electron microscopy of *Cpn* abberant bodies.

Some potential limitations to our study should be noted. There was only one biological replicate used for each strain of *Cpn*. All other replicates were technical replicates. Although there was a sample size of 6 or more per gene per time point studied, in order to increase the statistical significance, the study should be replicated with biological experimental replicates. In addition, we did not induce persistence with a model such as exposing the bacteria to IFN-γ. Having this data in comparison to the acute infection to compare and contrast would strengthen our findings. In addition, in future studies it would be important to visualize the organism within monocytes with electron microscopy and compare this to the genetic data. This information would help us determine a trend toward persistence, if we were able to visualize aberrant bodies.

4.1 Conclusions

In conclusion, our study helps contribute to the overall understanding of how *Cpn* interacts with its host. We still have a lot to learn about its interplay and only few studies have evaluated *Cpn* gene expression within a monocyte cell line (34, 45), a crucial component to the development of *Cpn* persistent infection and pathogenesis of AD. The purpose of this study was to investigate transcriptional gene changes of *Cpn* following infection of human THP1 monocytes over a 120-hour time course to evaluate potential evolution of an acute infection to that of a chronic infection. Our research demonstrates certain gene changes that are suggestive of progression towards chronic and perhaps persistent infection. In order to validate these findings, visualization of enlarged, morphologically aberrant *Cpn* bodies through ultrastructural analysis is needed. In addition, we would need more replication experiments to strengthen this study.

Previous studies have demonstrated that *Cpn* can establish a persistent infection within monocytes and lead to chronic inflammation (43). It has been proposed that monocytes can travel to distant anatomical sites, cross the blood brain barrier and produce neuroinflammation. This neuroinflammation leads to the neurodegeneration seen in LOAD (42). Therefore, an understanding of the evolution of acute to persistent *Cpn* infection within monocytes is crucial to our understanding of disease pathogenesis of LOAD.

Cpn gene expression within monocytes is still not well understood. Although genome wide transcriptional analyses have been studied within epithelial cell lines, monocytes are an important part of disease pathogenesis. Our study aids in this

understanding, however there is much to still be elucidated within this field. Continued research evaluating *Cpn* gene expression following infection of monocytes is crucial to understanding the evolution of acute to persistent infection. Genetic profiling of *Cpn* will help us better identify transcriptional patterns that are consistent with persistent *Cpn* infections. In addition, a better understanding of gene expression and regulation could potentially lead to treatments that could aid in eradicating persistent infections prior to them leading to disease pathology.

REFERENCES

1. Alzheimer's Association [Internet].; 2019 []. Available from: https://alz.org/.

2. Ballard C, Gauthier S, Corbett A, Brayne C, Aarsland D, Jones E. Alzheimer's disease. Lancet. 2011 Mar 19;377(9770):1019-31.

3. Balin BJ, Appelt DM. Role of infection in Alzheimer's disease. J Am Osteopath Assoc. 2001 Dec;101(12 Suppl Pt 1):1.

4. Tanzi RE. The genetics of Alzheimer disease. Cold Spring Harb Perspect Med. 2012 Oct 1;2(10):10.1101/cshperspect.a006296.

5. Tamaoka A. The pathophysiology of Alzheimer's disease with special reference to "amyloid cascade hypothesis". Rinsho Byori. 2013 Nov;61(11):1060-9.

6. McGeer PL, McGeer EG. The amyloid cascade-inflammatory hypothesis of Alzheimer disease: implications for therapy. Acta Neuropathol. 2013 Oct;126(4):479-97.

7. Dickson DW, Crystal HA, Mattiace LA, Masur DM, Blau AD, Davies P, et al. Identification of normal and pathological aging in prospectively studied nondemented elderly humans. Neurobiol Aging. 1992;13(1):179-89.

8. Soscia SJ, Kirby JE, Washicosky KJ, Tucker SM, Ingelsson M, Hyman B, et al. The Alzheimer's disease-associated amyloid beta-protein is an antimicrobial peptide. PLoS One. 2010 Mar 3;5(3):e9505.

9. Salomone S, Caraci Filippo, Marco Leggio G, Fedotova J, Drago F. New pharmacological strategies for treatment of Alzheimer's disease: focus on disease modifying drugs . 2012;73(4):504-17.

10. Meyer P, Tremblay-Mercier J, Leoutsakos J, Madjar C, Lafaille-Maignan M, Savard M, et al. INTREPAD. Neurology. 2019;92(18):e2070.

11. Breitner JC. The role of anti-inflammatory drugs in the prevention and treatment of Alzheimer's disease. Annu Rev Med. 1996;47:401-11.

12. Pasinetti GM. From epidemiology to therapeutic trials with anti-inflammatory drugs in Alzheimer's disease: the role of NSAIDs and cyclooxygenase in beta-amyloidosis and clinical dementia. J Alzheimers Dis. 2002 Oct;4(5):435-45.

13. Balin BJ, Hudson AP. Herpes viruses and Alzheimer's disease: new evidence in the debate. The Lancet Neurology. 2018;17(10):839-41.

14. Balin BJ, Hudson AP. Etiology and pathogenesis of late-onset Alzheimer's disease. Curr Allergy Asthma Rep. 2014 Mar;14(3):1.

15. Miklossy J. Historic evidence to support a causal relationship between spirochetal infections and Alzheimer's disease. Front Aging Neurosci. 2015 Apr 16;7:46.

16. Itzhaki RF. Corroboration of a Major Role for Herpes Simplex Virus Type 1 in Alzheimer's Disease. Frontiers in Aging Neuroscience. 2018;10:324.

17. Wozniak MA, Frost AL, Itzhaki RF. The helicase-primase inhibitor BAY 57-1293 reduces the Alzheimer's disease-related molecules induced by herpes simplex virus type 1. Antiviral Res. 2013 Sep;99(3):401-4.

18. Balin BJ, Gerard HC, Arking EJ, Appelt DM, Branigan PJ, Abrams JT, et al. Identification and localization of Chlamydia pneumoniae in the Alzheimer's brain. Med Microbiol Immunol. 1998 Jun;187(1):23-42.

19. Little CS, Joyce TA, Hammond CJ, Matta H, Cahn D, Appelt DM, et al. Detection of bacterial antigens and Alzheimer's disease-like pathology in the central nervous system of BALB/c mice following intranasal infection with a laboratory isolate of Chlamydia pneumoniae. Front Aging Neurosci. 2014 Dec 5;6:304.

20. Little CS, Hammond CJ, MacIntyre A, Balin BJ, Appelt DM. Chlamydia pneumoniae induces Alzheimer-like amyloid plaques in brains of BALB/c mice. Neurobiol Aging. 2004 Apr;25(4):419-29.

21. Abdelrahman YM, Belland RJ. The chlamydial developmental cycle. FEMS Microbiol Rev. 2005 Nov;29(5):949-59.

22. Maurer AP, Mehlitz A, Mollenkopf HJ, Meyer TF. Gene expression profiles of Chlamydophila pneumoniae during the developmental cycle and iron depletion-mediated persistence. PLoS Pathog. 2007 Jun;3(6):e83.

23. Aistleitner K, Anrather D, Schott T, Klose J, Bright M, Ammerer G, et al. Conserved features and major differences in the outer membrane protein composition of chlamydiae. Environ Microbiol. 2015 Apr;17(4):1397-413.

24. Grayston JT, Aldous MB, Easton A, Wang SP, Kuo CC, Campbell LA, et al. Evidence that Chlamydia pneumoniae causes pneumonia and bronchitis. J Infect Dis. 1993 Nov;168(5):1231-5.

25. Campbell LA, Yaraei K, Van Lenten B, Chait A, Blessing E, Kuo CC, et al. The acute phase reactant response to respiratory infection with Chlamydia pneumoniae: implications for the pathogenesis of atherosclerosis. Microbes Infect. 2010 Aug;12(8-9):598-606.

26. Nagy A, Keszei M, Kis Z, Budai I, Tolgyesi G, Ungvari I, et al. Chlamydophila pneumoniae infection status is dependent on the subtypes of asthma and allergy. Allergy Asthma Proc. 2007;28(1):58-63.

27. Chu DJ, Guo SG, Pan CF, Wang J, Du Y, Lu XF, et al. An experimental model for induction of lung cancer in rats by Chlamydia pneumoniae. Asian Pac J Cancer Prev. 2012;13(6):2819-22.

28. Rizzo A, Domenico MD, Carratelli CR, Paolillo R. The role of Chlamydia and Chlamydophila infections in reactive arthritis. Intern Med. 2012;51(1):113-7.

29. Tang LF, Wang DF, Cao LQ, Wu XD, Lu J, Yu FF. Correlation between Chlamydia pneumoniae infection and chronic obstructive pulmonary disease. Zhonghua Liu Xing Bing Xue Za Zhi. 2012 Oct;33(10):1072-4.

30. Rodriguez AR, Plascencia-Villa G, Witt CM, Yu JJ, Jose-Yacaman M, Chambers JP, et al. Chlamydia pneumoniae promotes dysfunction of pancreatic beta cells. Cell Immunol. 2015 Apr 1;295(2):83-91.

31. MacIntyre A, Abramov R, Hammond CJ, Hudson AP, Arking EJ, Little CS, et al. Chlamydia pneumoniae infection promotes the transmigration of monocytes through human brain endothelial cells. J Neurosci Res. 2003 Mar 1;71(5):740-50.

32. Itzhaki RF, Wozniak MA. Alzheimer's disease, the neuroimmune axis, and viral infection. J Neuroimmunol. 2004 Nov;156(1-2):1-2.

33. Velayudhan L, Gasper A, Pritchard M, Baillon S, Messer C, Proitsi P. Pattern of Smell Identification Impairment in Alzheimer's Disease. J Alzheimers Dis. 2015 Mar 10.

34. Mannonen L, Kamping E, Penttila T, Puolakkainen M. IFN-gamma induced persistent Chlamydia pneumoniae infection in HL and Mono Mac 6 cells: characterization by real-time quantitative PCR and culture. Microb Pathog. 2004 Jan;36(1):41-50.

35. Byrne GI, Ouellette SP, Wang Z, Rao JP, Lu L, Beatty WL, et al. Chlamydia pneumoniae expresses genes required for DNA replication but not cytokinesis during persistent infection of HEp-2 cells. Infect Immun. 2001;69(9):5423-9.

36. Belland RJ, Nelson DE, Virok D, Crane DD, Hogan D, Sturdevant D, et al. Transcriptome analysis of chlamydial growth during IFN-gamma-mediated persistence and reactivation. Proc Natl Acad Sci U S A. 2003 Dec 23;100(26):15971-6.

37. Chacko A, Beagley KW, Timms P, Huston WM. Human Chlamydia pneumoniae isolates demonstrate ability to recover infectivity following penicillin treatment whereas

animal isolates do not. FEMS Microbiol Lett. 2015 Mar;362(6):10.1093/femsle/fnv015. Epub 2015 Feb 5.

38. Al-Younes HM, Rudel T, Brinkmann V, Szczepek AJ, Meyer TF. Low iron availability modulates the course of Chlamydia pneumoniae infection. Cell Microbiol. 2001 Jun;3(6):427-37.

39. Ringheim GE, Conant K. Neurodegenerative disease and the neuroimmune axis (Alzheimer's and Parkinson's disease, and viral infections). J Neuroimmunol. 2004 Feb;147(1-2):43-9.

40. Griffin WS, Sheng JG, Royston MC, Gentleman SM, McKenzie JE, Graham DI, et al. Glial-neuronal interactions in Alzheimer's disease: the potential role of a 'cytokine cycle' in disease progression. Brain Pathol. 1998 Jan;8(1):65-72.

41. Swardfager W, Lanctot K, Rothenburg L, Wong A, Cappell J, Herrmann N. A meta-analysis of cytokines in Alzheimer's disease. Biol Psychiatry. 2010 Nov 15;68(10):930-41.

42. McGeer PL, McGeer EG. Local neuroinflammation and the progression of Alzheimer's disease. J Neurovirol. 2002 Dec;8(6):529-38.

43. Lim C, Hammond CJ, Hingley ST, Balin BJ. Chlamydia pneumoniae infection of monocytes in vitro stimulates innate and adaptive immune responses relevant to those in Alzheimer inverted question marks disease. J Neuroinflammation. 2014 Dec 24;11(1):5.

44. Ouellette SP, Hatch TP, AbdelRahman YM, Rose LA, Belland RJ, Byrne GI. Global transcriptional upregulation in the absence of increased translation in Chlamydia during IFNγ-mediated host cell tryptophan starvation. Mol Microbiol. 2006;62(5):1387-401.

45. Mannonen L, Markkula E, Puolakkainen M. Analysis of Chlamydia pneumoniae infection in mononuclear cells by reverse transcription-PCR targeted to chlamydial gene transcripts. Med Microbiol Immunol. 2011 Aug;200(3):143-54.

46. Read TD, Brunham RC, Shen C, Gill SR, Heidelberg JF, White O, et al. Genome sequences of Chlamydia trachomatis MoPn and Chlamydia pneumoniae AR39. Nucleic Acids Res. 2000 Mar 15;28(6):1397-406.

47. Mäurer A,P., Mehlitz A, Mollenkopf HJ, Meyer TF. Gene Expression Profiles of Chlamydophila pneumoniae during the Developmental Cycle and Iron Depletion–Mediated Persistence. PLOS Pathogens. 2007;3(6):e83.

48. Shen L, Shi Y, Douglas AL, Hatch TP, O'Connell CMC, Chen J, et al. Identification and Characterization of Promoters Regulating tuf Expression in Chlamydia trachomatis Serovar F. Archives of Biochemistry and Biophysics. 2000;379(1):46-56.

49. Rosario CJ, Hanson BR, Tan M. The transcriptional repressor EUO regulates both subsets of Chlamydia late genes. Mol Microbiol. 2014 Nov;94(4):888-97.

50. Polkinghorne A, Hogan RJ, Vaughan L, Summersgill JT, Timms P. Differential expression of chlamydial signal transduction genes in normal and interferon gamma-induced persistent Chlamydophila pneumoniae infections. Microb Infect. 2006;8(1):61-72.

51. Watson MW, Clarke IN, Everson JS, Lambden PR. The CrP operon of Chlamydia psittaci and Chlamydia pneumoniae. Microbiology. 1995;141(10):2489-97.

52. Hogan RJ, Mathews SA, Kutlin A, Hammerschlag MR, Timms P. Differential expression of genes encoding membrane proteins between acute and continuous Chlamydia pneumoniae infections. Microb Pathog. 2003;34(1):11-6.

53. Boelen E, Stassen FR, van der Ven, A. J., Lemmens MA, Steinbusch HP, Bruggeman CA, et al. Detection of amyloid beta aggregates in the brain of BALB/c mice after Chlamydia pneumoniae infection. Acta Neuropathol. 2007 Sep;114(3):255-61.

54. Barry CE,3rd, Brickman TJ, Hackstadt T. Hc1-mediated effects on DNA structure: a potential regulator of chlamydial development. Mol Microbiol. 1993 Jul;9(2):273-83.

55. Tattersall J, Rao GV, Runac J, Hackstadt T, Grieshaber SS, Grieshaber NA. Translation inhibition of the developmental cycle protein HctA by the small RNA IhtA is conserved across Chlamydia. PloS one. 2012;7(10):e47439.

56. Barry CE, Hayes SF, Hackstadt T. Nucleoid Condensation in *Escherichia coli* That Express a Chlamydial Histone Homolog. Science. 1992;256(5055):377.

57. Di Pietro M, Tramonti A, De Santis F, De Biase D, Schiavoni G, Filardo S, et al. Analysis of gene expression in penicillin G induced persistence of Chlamydia pneumoniae. J Biol Regul Homeost Agents. 2012;26(2):277-84.

58. Beth P. Goldstein 1, Giuseppina Zaffaroni 1, Orsola Tiboni 2 Bozorgmehr Amiri 1 and Maurizio Denaro I. Determination of the number of tuf genes in Chlamydia trachomatis and Neisseria gonorrhoeae. FEMS Microbiology Letters. 1989 10 April(60):305-10.

59. Blocker A, Komoriya K, Aizawa S. Type III secretion systems and bacterial flagella: Insights into their function from structural similarities. Proc Natl Acad Sci USA. 2003;100(6):3027.

60. Slepenkin A, Motin V, de lM, Peterson EM. Temporal Expression of Type III Secretion Genes of *Chlamydia pneumoniae*. Infect Immun. 2003;71(5):2555.

APPENDIX

5.1 Additional Material and Methods: DNA Isolation

DNA was purified according to the manufacturer's instructions using a DNeasy isolation kit (Qiagen DNeasy). Frozen pellets were thawed and centrifuged for 5 min at 300 x g. Pellets contained $1x10^6$ cells was for each sample. 150 µL of PBS, 20 µL of proteinase K, and 200 µL of Buffer AL was added to sample and vortexed thoroughly followed by incubation in a water bath for 10 min at 56 °C. After incubation, 200 µL of ethanol was added to each sample and vortexed to yield a homogeneous solution. The entire mixture was then pipetted into a DNeasy Mini spin column placed in a 2mL collection tube. Each sample was centrifuged for 1 min at 6000xg. The flow through and collection tube was discarded and the DNeasy spin column was placed in new collection tube. 500ul of Buffer AW1 was added to the spin column and centrifuged for 1 min at 6000xg. Flow through and collection tube were discarded and the DNeasy spin column was placed in new collection tube. 500ul of Buffer AW2 was added to the spin column and centrifuged for 3 min at 20,000xg to dry the DNeasy membrane. Flow through and collection tube were discarded and DNeasy spin column was placed in new collection tube. Sample was centrifuged again for 1 min at 20,000xg to ensure all ethanol was evaporated from spin column. Flow through and collection tube were discarded and the DNeasy spin column was placed in a 2ml microcentrifuge tube. 100ul of Buffer AE was pipetted into the column and centrifuged for 1 min at 6000xg. This step was repeated for a total of 200ul of eluted DNA in Buffer AE. Samples were frozen and stored at -60°C until DNA was used for RT-PCR.

After DNA isolation was performed, overall DNA yield was determined by using UV Spectrophotometry. Other measurements recorded included purity values: A_{260}:A_{230} and A_{260}: A_{280}.

5.2 LIST OF APPENDIX TABLES

Table 3. Results of *abcX* gene expression following infection of THP 1 Human Monocytes with two different *Cpn* strains AR39 and CWL02942.....41

Table 4. Results of *abcX* gene expression following infection of THP 1 Human Monocytes with two different *Cpn* strains AR39 and CWL02942.....41

Table 5. Results of *euo* gene expression following infection of THP 1 Human Monocytes with two different *Cpn* strains AR39 and CWL02942.....42

Table 6. Results of *euo* gene expression following infection of THP 1 Human Monocytes with two different *Cpn* strains AR39 and CWL02942.....42

Table 7. Results of *abcX* gene expression following infection of THP 1 Human Monocytes with two different *Cpn* strains AR39 and CWL02942.....43

Table 8. Results of *abcX* gene expression following infection of THP 1 Human Monocytes with two different *Cpn* strains AR39 and CWL02942.....43

5.3 Additional Results

5.3.1 *abcX* qRT-PCR raw data

AR39	RQ value at 24 hpi	RQ value at 48 hpi	RQ value at 72 hpi	RQ value at 96 hpi	RQ value at 120 hpi
Plate 022415	2.61	1.00	0.47	1.03	***
Plate 031615	3.24	1.00	1.08	0.42	0.63
Mean	2.93	1.00	0.78	0.73	N/A
SD	0.45	0.00	0.43	0.43	N/A

Table 3

CWL029	RQ value at 24 hpi	RQ value at 48 hpi	RQ value at 72 hpi	RQ value at 96 hpi	RQ value at 120 hpi
Plate 030915	1.41	1.00	0.45	0.33	0.42
Plate 031615	0.78	1.00	3.09	1.07	0.69
Mean	1.10	1.00	1.77	0.70	0.56
SD	0.45	0.00	1.87	0.52	0.19

Table 4

Table 3 and 4. Results of *abcX* gene expression following infection of THP 1 Human Monocytes with two different Cpn strains AR39 and CWL029. Cells were infected separately (MOI 1) with *Cpn*. Cells were lysed and RNA was extracted at 24, 48, 72, 96, and 120 hpi. 48 hpi was used as a reference time point and *18S* was used as a chlamydial housekeeping gene to normalize transcription levels. Relative quantity (RQ) refers to the gene expression level after RT-PCR (Real Time PCR). Individual experiments were performed with 3 technical replicates. *** represents gene targets that did not amplify and therefore no RQ values were obtained.

5.3.2 *euo* qRT-PCR raw data

AR39	RQ value at 24 hpi	RQ value at 48 hpi	RQ value at 72 hpi	RQ value at 96 hpi	RQ value at 120 hpi
Plate 021815	4.44	1.00	1.47	0.35	1.35
Plate 031815	6.43	1.00	4.73	2.78	2.96
Mean	5.44	1.00	3.10	1.57	2.16
SD	1.41	0.00	2.31	1.72	1.14

Table 5

CWL029	RQ value at 24 hpi	RQ value at 48 hpi	RQ value at 72 hpi	RQ value at 96 hpi	RQ value at 120 hpi
Plate 031115	0.75	1.00	1.08	2.35	2.01
Plate 031815	0.74	1.00	***	1.11	0.28
Mean	0.75	1.00	N/A	1.73	1.15
SD	0.01	0.00	N/A	0.88	1.22

Table 6

Table 5 and 6. Results of *euo* gene expression following infection of THP 1 Human Monocytes with two different Cpn strains AR39 and CWL029. Cells were infected separately (MOI 1) with *Cpn*. Cells were lysed and RNA was extracted at 24, 48, 72, 96, and 120 hpi. 48 hpi was used as a reference time point and *18S* was used as a chlamydial housekeeping gene to normalize transcription levels. Relative quantity (RQ) refers to the gene expression level after RT-PCR (Real Time PCR). Individual experiments were performed with 3 technical replicates. *** represents gene targets that did not amplify and therefore no RQ values were obtained.

5.3.3 *l29* qRT-PCR raw data

AR39	RQ value at 24 hpi	RQ value at 48 hpi	RQ value at 72 hpi	RQ value at 96 hpi	RQ value at 120 hpi
Plate	1.79	1.00	1.26	0.19	0.46
Plate 031815	0.64	1.00	0.9	0.16	***
Mean	1.22	1.00	1.08	0.18	N/A
SD	0.81	0.00	0.25	0.02	N/A

Table 7

CWL029	RQ value at 24 hpi	RQ value at 48 hpi	RQ value at 72 hpi	RQ value at 96 hpi	RQ value at 120 hpi
Plate 031115	0.59	1.00	1.21	1.03	0.82
Plate 031815	2.19	1.00	***	0.55	0.36
Mean	1.39	1.00	N/A	0.79	0.59
SD	1.13	0.00	N/A	0.34	0.33

Table 8

Table 7 and 8. Results of *l29* gene expression following infection of THP 1 Human Monocytes with two different Cpn strains AR39 and CWL029. Cells were infected separately (MOI 1) with *Cpn*. Cells were lysed and RNA was extracted at 24, 48, 72, 96, and 120 hpi. 48 hpi was used as a reference time point and *18S* was used as a chlamydial housekeeping gene to normalize transcription levels. Relative quantity (RQ) refers to the gene expression level after RT-PCR (Real Time PCR). Individual experiments were performed with 3 technical replicates. *** represents gene targets that did not amplify and therefore no RQ values were obtained.